

# NOON STATE AND ITS APPLICATIONS



A thesis submitted towards partial fulfilment of  
BS-MS Dual Degree Programme

by

C. LALTLANZUALA

under the guidance of

DR T S MAHESH

ASSOCIATE PROFESSOR, IISER-PUNE

INDIAN INSTITUTE OF SCIENCE EDUCATION AND RESEARCH  
PUNE

# Certificate

This is to certify that this thesis entitled "N00N State and its Applications" submitted towards the partial fulfilment of the BS-MS dual degree programme at the Indian Institute of Science Education and Research Pune represents original research carried out by C. LALTLANZUALA at INDIAN INSTITUTE OF SCIENCE EDUCATION AND RESEARCH, PUNE under the supervision of Dr T S MAHESH during the academic year 2014-2015.



Student  
C. LALTLANZUALA



Supervisor  
DR. T S MAHESH

# Declaration

I hereby declare that the matter embodied in the report entitled "N00N State and its Applications" are the results of the investigations carried out by me at the Department of Physics, Indian Institute of Science Education and Research, Pune under the supervision of Dr. T S Mahesh and the same has not been submitted elsewhere for any other degree.



Student  
C. LALTLANZUALA



Supervisor  
DR T S MAHESH

# Acknowledgements

First of all, I would like to thank my supervisor Dr. T S Mahesh, who has spent enormous effort and guiding me throughout the entire year and offer me uncountable number of help in my work for the completion of my thesis and Dr. Jitender Chugh, for being a key role in my Thesis Advisory Committee . Also, a lot of my gratitude is on Abhishek Shukla, Phd student under Dr. T S Mahesh who has been assisting me in my project work and willing to help whenever necessary, and my lab mates, namely, Swathi Hegde, Deepak Khurana, C S Sudheer Kumar, Anjusha V S and my batchmate Krishna Sriram, who were helping me in all the queries I had, thanks to all those teachers, from whom I gain tremendous amount of knowledge and skills during my course work semesters. Lastly, but not the least, thanks to my parents, relatives for supporting me throughout my entire life in IISER-Pune and above all, my heavenly God, who has showered His endless grace upon me.

# Abstract

This Thesis is focussed on the preparation and applications of multiple quantum coherence such as MSSM (Many some, + Some many) States and N00N state (quantum mechanical many-body entangled state) in star topology molecules such as Trimethylphosphite (TMP) and Triisopropylphosphite, where  $|0100\rangle + |1011\rangle$ , where  $|0\rangle$  denotes spin up and  $|1\rangle$  denotes spin down, is a particular example of MSSM for four spin  $\frac{1}{2}$  system and the N00N State can be represented by  $|\Psi_{N00N}\rangle = \frac{1}{\sqrt{2}}(|N_{\uparrow}, 0_{\downarrow}\rangle + |0_{\uparrow}, N_{\downarrow}\rangle)$  (*N spins up, zero spin down + zero spin up, N spins down*), where  $N$  is the number of spins. The technique of preparing multiple quantum coherence is used to study slow diffusion of TMP in liquid crystal EBBA and the N00N state has been generated in both the molecules. Also, we demonstrate how spin polarisation transfer from one nucleus which has higher gyromagnetic ratio to other nucleus (with lower gyromagnetic ratio) using Insensitive Nuclear Enhancement by Polarisation Transfer (INEPT) can enhance the signal of the nucleus to which spin polarisations are transferred.

# Contents

<b>1</b>	<b>Introduction</b>	<b>3</b>
1.1	The History . . . . .	3
1.2	About N00N state . . . . .	3
<b>2</b>	<b>Theory</b>	<b>4</b>
2.1	About NMR . . . . .	4
2.1.1	Diffusion . . . . .	5
2.1.2	Hahn Echo . . . . .	5
2.2	Basis of Pulse Field Gradient(PFG) NMR . . . . .	6
2.2.1	Effects of field gradients on Spin Precession . . . . .	7
2.2.2	Qualitative analysis of Hahn Echo Attenuation . . . . .	8
<b>3</b>	<b>Experimental Section</b>	<b>11</b>
3.1	Theoretical Background . . . . .	11
3.1.1	Measurement of Diffusion Constant . . . . .	13
3.1.2	Experimental part for Diffusion . . . . .	14
3.2	Generating different N00N state in 22 spin system . . . . .	16
3.2.1	Experimental Part for N00N states . . . . .	17
3.2.2	Coherence selection by field gradients . . . . .	18
<b>4</b>	<b>Results</b>	<b>19</b>
4.1	Data of diffusion experiment . . . . .	19
4.1.1	Calculations of Diffusion constant for different quantum coherences . . . . .	24
4.2	Pulse sequence and Signal Spectrum of N00N states . . . . .	25
<b>5</b>	<b>Discussion</b>	<b>27</b>
5.1	Comparison between single quantum diffusion and multiple quantum diffusion . . . . .	27
5.2	N00N states . . . . .	27

<b>References</b>	<b>28</b>
<b>A Long proofs</b>	<b>30</b>
A.1 Proof of Hahn Echo described in Sec 2.1.2 using product operator formalism . . . . .	30
A.2 Effect of Pulse Field Gradient on Hahn Echo in presence of diffusion . . . . .	33
A.3 Insensitive Nuclei Enhanced by Polarization Transfer(INEPT)	35
A.3.1 Background . . . . .	35
A.3.2 INEPT technique . . . . .	35
A.4 List of figures and tables . . . . .	36

# Chapter 1

## Introduction

### 1.1 The History

The potential application of Nuclear Magnetic Resonance Spectroscopy has been explored to a great extent. Among them are in studying the diffusion of molecules in different media using radio frequency pulses and magnetic field gradients (also called PFG NMR) through the concept called "Hahn Echo", which is the refocusing of the nuclear spin magnetization, discovered by Erwin Hahn in 1950 [1]. The PFG NMR method was first explained theoretically and experimentally by Stejskal and Tanner[2] and is widely used till today to obtain the information about molecular dynamics, especially longitudinal diffusion. The diffusion of molecules in the medium are studied by monitoring the intensity of the Hahn Echo signal by varying the strength of the magnetic field gradient. Using the mathematical relationship between the intensity of the Hahn Echo signal and the gradient strength, the value of the diffusion constant "D" of the molecules can be determined for different media, which is the major part of our work .

### 1.2 About N00N state

Another application of Nuclear Magnetic Resonance is the generation of N00N states in large molecules, which is the quantum mechanical many-body entangled state. This has been done by using quantum logic gates, mainly Hadamard and Control-Not(C-NOT) gates and selective magnetic field gradients. The purpose of the selective gradients is to extract the specific N00N signal from the spectrum. The molecule that we have used for generating N00N state is tri-isopropyl-phosphite, which is of 22 spin system. We had also used this technique to study the diffusion of molecules.



# Chapter 2

## Theory

This chapter contains a short introduction about Nuclear Magnetic Resonance(NMR), the theoretical explanation of how diffusion is studied and the method applied to determine the diffusion constant  $D$ .

### 2.1 About NMR

The principle of NMR utilises the magnetic moment generated by nuclear spin, which is given by  $\hat{\mu} = \gamma\hat{I}$ , where  $\gamma$  is the gyromagnetic ratio and  $\hat{I}$  is the spin angular momentum of the nucleus. Since most nucleus used in NMR are spin  $\frac{1}{2}$  ( $I = \frac{1}{2}$ ), for these nuclei, there are two Zeeman eigenstates : spin up, denoted by  $|0\rangle$  and spin down, denoted by  $|1\rangle$ . On applying a very strong external magnetic field along the  $z$  direction(generally upward), the degeneracy of the Zeeman states breaks down, with  $|0\rangle$  being in the lower energy state and  $|1\rangle$  in the higher energy state. Due to this, the nuclei in the sample attains equilibrium distribution, with more population in the lower energy state than the higher energy state, this results in net magnetization along the external field and the energy separation between the states lies in the radio frequency range.

The external field also causes the nuclei to precess about the  $z$  axis. This precession is called Larmor precession and the frequency is called Larmor frequency, given by  $\omega_o = -\gamma B_o$ , where  $B_o$  is the strength of the external field in tesla, and the minus sign indicates the sense of the spin precession around the applied field. Most nuclei have positive  $\gamma$ , in this case the Larmor frequency is negative. This means that the precession is in the clockwise direction, as seen when looking against the direction of the applied field. For nuclei which have positive  $\gamma$ , their Larmor frequency is positive, and their precession is in the anti-clockwise direction, as seen against the direction of

the applied field. To excite the nuclei, an on resonant radio frequency(RF) is applied to the nuclei, this flips the equilibrium magnetization away from the equilibrium position to the transverse plane, and the flip angle depends on the time duration and strength of the RF field. The rotation of the magnetization in the transverse plane generates an oscillating magnetic field and this oscillating field is converted into electrical signal by using probe coils. This electrical signal is called Free Induction Decay(FID) which is in the time domain. To convert it to frequency domain, the FID is Fourier Transformed to give the precession frequency of the magnetization.

### 2.1.1 Diffusion

The self diffusion of molecules or ions is mainly caused by the internal energy[3]. Translational diffusion is the process through which molecules spread around in space. This phenomenon has a connection with structural properties of the diffusing molecules, because the diffusion constants  $D$  depend on frictional factors and effective charges. In the absence of thermal or concentration gradients, the average molecular displacement in all directions is zero, but not the mean square displacement, given by  $\langle r^2 \rangle = 6Dt$ [4],  $t$  being the diffusion time. From the Stokes-Einstein equation[5],

$D = \frac{k_B T}{f}$ , where  $k_B$  is the Boltzman constant,  $T$  is the temperature and  $f = 6\pi\eta r$  ( $\eta =$  viscosity of the medium and  $r =$  radius of the particle) is the friction factor obtained from Stoke's law[6].

NMR technique is suitable to study such molecular dynamics, and the self diffusion data provide information about molecular organization and structural properties. Molecular diffusion is sensitive to structural properties and the ability of the molecule to bind and associate with the medium and the values of diffusion constant are in proportion to the rate of molecular displacement[4].

### 2.1.2 Hahn Echo

As mentioned in the introduction, Hahn Echo is the underlying principle for studying diffusion. The concept of this echo was introduced by Erwin Hahn[1] and the pulse sequence is shown in figure 2.1. First, a  $90^\circ$  pulse is applied along the  $X$ -axis, this rotates the magnetization vector from the  $Z$ -axis to the  $-Y$  axis (fig 2.2(B)), during the free evolution(absence of RF) of duration  $\tau$ , the magnetization vector precesses in the  $X - Y$  plane. Due to the local field inhomogeneities experienced by each spin, also called chemical shift, the spins dephase as a result, the transverse magnetization vector starts

fading out as shown in figure 2.2(C). At the end of time  $\tau$ , a  $180^\circ$  pulse is applied along the  $X$  axis, which rotates the spins by  $180^\circ$  about the  $X$  axis and remain in the  $X - Y$  plane, and since each spin continues to precess with its own frequency, all spins are rephased and the transverse magnetization is regained after time duration of  $\tau$  from the  $180^\circ$  pulse, forming an echo (fig 2.2). The importance of the Hahn Echo is that it nullifies the effects due to local field inhomogeneities.

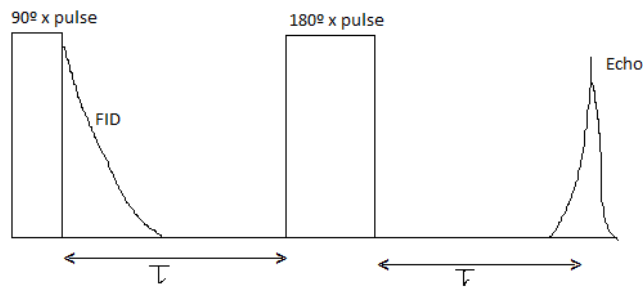


Figure 2.1: Hahn Echo pulse

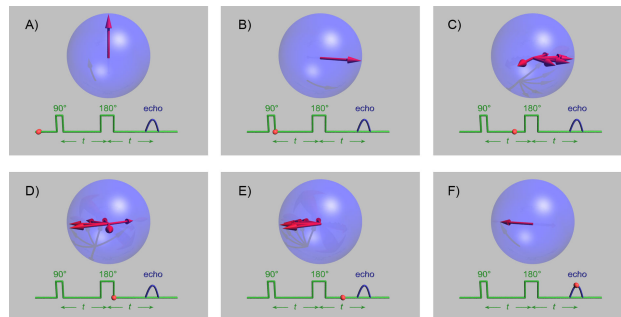


Figure 2.2: Pictorial illustration of Hahn Echo, image taken from source:[http://en.wikipedia.org/wiki/Spin\\_echo#mediaviewer/File:SpinEcho\\_GWM\\_stills.jpg](http://en.wikipedia.org/wiki/Spin_echo#mediaviewer/File:SpinEcho_GWM_stills.jpg)

## 2.2 Basis of Pulse Field Gradient(PFG) NMR

In the PFG- NMR experiments, apart from the RF pulses, magnetic field gradients[2, 7] are introduced along the main magnetic field  $B_0$  (fig 2.3). All NMR diffusion measurements are based on the fact that the diffusion constant  $D$  can be calculated from the Hahn Echo attenuation, if the duration and strength of the gradients are known.

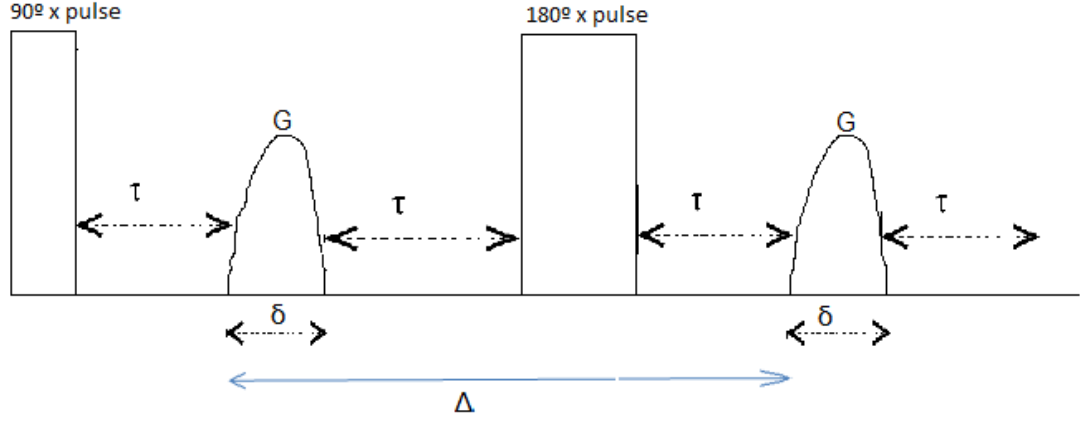


Figure 2.3: Pulse sequence of PFG NMR,  $\delta$  is the duration of the gradient and  $\Delta$  is called the diffusion time,  $G$  is the gradient strength.

### 2.2.1 Effects of field gradients on Spin Precession

To explain the effects of magnetic field gradients on nuclear spin, we need to start from the Larmor equation[4, 8]:

$$\omega_o = -\gamma B_o \quad (2.1)$$

where  $\gamma$  is the gyromagnetic ratio and  $B_o$  is the strength of the static external field which is homogenous over the sample in time and space. When additional field which has spatial variation along the vertical axis  $B(z)$ , called field gradient is introduced, then the total magnetic field at a point  $z$  inside the sample is:

$$B(z) = B_o + Gz \quad (2.2)$$

where  $G$  is the strength of the gradient. The role of the field gradient is to encode the spins with the phase angles that depend on their displacement in the  $z$ - direction since the Larmor frequency becomes spatially dependent on the application of gradient, given as:

$$\omega_z = -\gamma B(z) \quad (2.3)$$

As a result, the phase acquired by a spin with displacement  $z$  due to a  $z$  gradient of duration  $\delta$  is given by:

$$\phi(z) = \omega_z \delta \quad (2.4)$$

After the first pulse gradient, the phase shift of the spin at position  $z_1$  is:

$$\phi_1 = \phi_0 + \gamma \int Gz dt = \gamma Gz_1 \delta \quad (2.5)$$

where  $\phi_0$  is the initial phase before the first gradient. If the spin undergoes diffusion and is at position  $z_2$  when the second gradient is applied, the extra phase acquired is:

$$d\phi = \gamma \delta G(z_2 - z_1) \quad (2.6)$$

The total phase acquired at position  $z_2$  is:

$$\phi_2 = \phi_1 + d\phi = \phi_0 + \gamma \delta G(z_2 - z_1) \quad (2.7)$$

Due to this position dependent phase caused by the field gradients, the spins in different positions of the sample precess with different frequencies and enhance the dephasing process. If the spins retain their position throughout the pulse sequence, or technically speaking, if there is no diffusion at all, all their phases will be refocused completely after time  $\tau$  from the second gradient, since  $d\phi$  in eqn(2.7) is zero because  $z_1 = z_2$  and Hahn Echo will be achieved(left side of figure 2.4). But if the spins diffuse through the sample during the course of the pulse sequence, their phases will not be refocused completely, as seen in eqn(2.7) and complete Hahn Echo will not be achieved, causing a decrease in the intensity of the Echo signal(right side of figure 2.4)

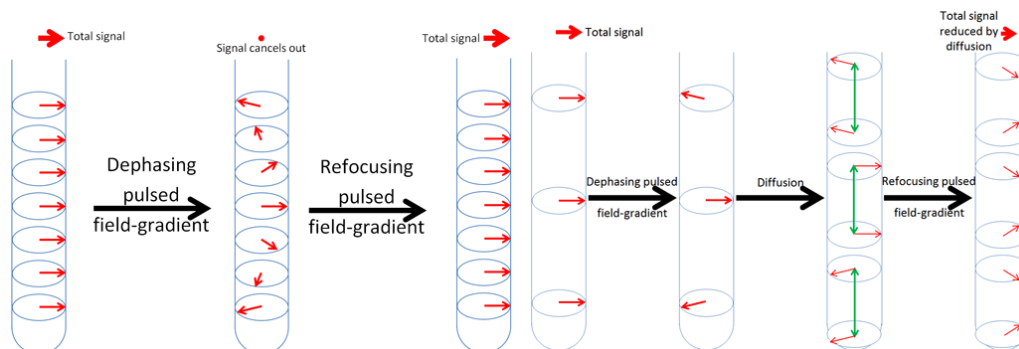


Figure 2.4: Effect of Gradient pulse on Hahn Echo with no diffusion(left side) and with diffusion(right side)

source:<http://chem.ch.huji.ac.il/nmr/techniques/other/diff/diff.html>

## 2.2.2 Qualitative analysis of Hahn Echo Attenuation

To describe the mechanism of signal attenuation in PFG NMR diffusion experiments, we need to start from the complex transverse magnetization

$M_{xy} = M_x + iM_y$ . Combining the Bloch equations with Fick's second law gives[4, 9, 10]:

$$\frac{\partial M_{xy}}{\partial t} = -i\omega_o M_{xy} - \frac{M_{xy}}{T_2} - i\gamma Gz M_{xy} + D\nabla^2 M_{xy} \quad (2.8)$$

From the mathematical point of view, the transverse magnetization can be written as:

$$M_{xy} = \psi(z, t) \exp(i\omega_o t - \frac{t}{T_2}) \quad (2.9)$$

to include the transverse relaxation term  $T_2$ . Substituting eqn. (2.9) into (2.8) we get

$$\frac{\partial \psi(z, t)}{\partial t} = -i\gamma Gz \psi(z, t) + D\nabla^2 \psi(z, t) \quad (2.10)$$

Setting

$$\psi(z, t) = \psi(t) \exp(-i\gamma z \int_0^t G dt') \quad (2.11)$$

and by substituting eqn (2.11) into (2.10), we get the solution to be:

$$\psi(t) = \psi(0) \exp[-D\gamma^2 \int_0^t (\int_0^t G dt'')^2 dt'] \quad (2.12)$$

The last equation can also be written as

$$\ln[\frac{S(t)}{S(0)}] = -D\gamma^2 \int_0^t (\int_0^t G dt'')^2 dt' \quad (2.13)$$

where  $S(t)$  and  $S(0)$  are the signal intensity at time  $t$  with and without magnetic field gradients i.e.  $S(0)$  is the signal just after  $90^\circ$  RF pulse, or echo signal amplitude in absence of gradient and is maximum in intensity which is taken to be 1 in calculations.

For the pulse sequence shown in fig 2a, the echo amplitude can be written as (ref eo stejkal):

$$S(t) = S(0) \exp(\frac{-4\tau}{T_2}) \exp[-D\gamma^2 G^2 \delta^2 (\Delta - \frac{\delta}{3})] \quad (2.14)$$

The correction term  $\delta/3$  is a result of the shape of the gradient pulses, where  $\delta$  is the duration of the gradient and  $\Delta$  is the time interval between the two gradients, and  $D$  being the diffusion constant.

From eqn (2.14), taking  $S(0) = 1$  and natural logarithm on both sides we get:

$$\ln[S(t)] = -D\gamma^2 G^2 \delta^2 (\Delta - \frac{\delta}{3}) \quad (2.15)$$

Here, we assume that  $T_2 \gg \tau$ . From this equation, we can plot the graph of  $\ln[S(t)]$  versus  $G^2$ , whose slope is  $-D\gamma^2\delta^2(\Delta - \frac{\delta}{3})$ , by fitting a linear plot to the data, we can calculate the value of  $D$ . The major advantages of an echo sequence with pulsed gradients are[10]:

1. The gradient pulse areas can be controlled independently of the time for the echo and
2. The signal can be read out in a homogenous magnetic field.

# Chapter 3

## Experimental Section

### 3.1 Theoretical Background

(Most of the texts/words and mathematical equations in this section are incorporated from the work already done by Abhishek Shukla et al[11]).

The approach that we used in this experiment is inspired by quantum information theory[12] and the use of multiple quantum[13] to speed up the measurement of diffusion constant through entangled spins in a star topology which is trimethylphosphite, since it has one central phosphorus and nine chemical and magnetically equivalent peripheral hydrogens. The circuit for generating entangled states and studying their diffusion is given below[11]:

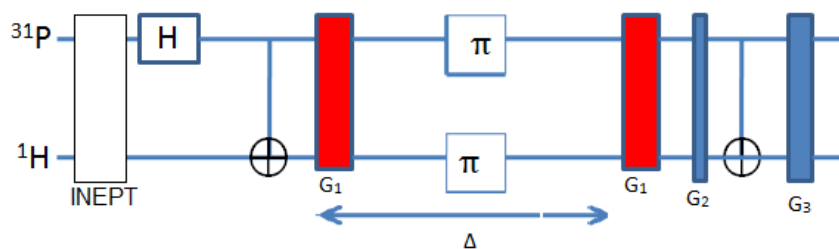


Figure 3.1: Circuit for generating and studying entangled states and their diffusion. INEPT (pulse diagram is given in fig A.1) is the technique used to transfer the spin polarization from hydrogens to phosphorus to increase the sensitivity of the central phosphorus spin. The capital "H" inside the rectangular box is the Hadamard operator, perpendicularly crossed circle is the control Not(C-NOT) gate  $G_1$  is the field gradient for studying diffusion,  $G_2$  and  $G_3$  are the selective gradients, their purpose is to select a particular coherence.



The pulse sequence for the circuit (fig 3.1) for studying diffusion is given under [11]:

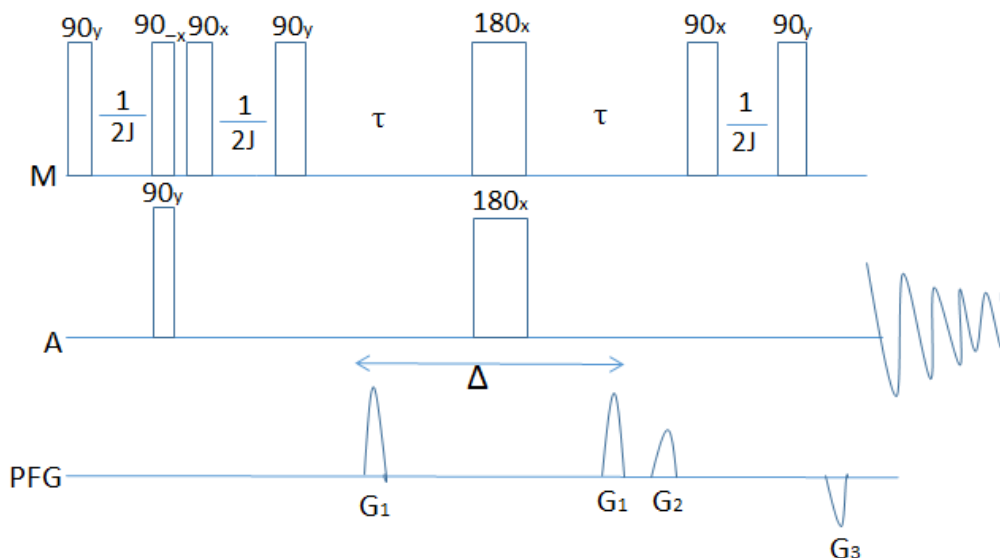


Figure 3.2: Pulse sequence for the circuit given in 3.1, A is the Phosphorus, M represents the 9 peripheral hydrogens,  $\Delta$  is called the diffusion time, the C-NOT gate is implemented using  $90_x^0$  pulse followed  $90_y^0$  pulse with  $\frac{1}{2J}$  time interval in between. In this experiment instead of actual Hadamard operator, pseudo Hadamard operator is used which is  $90_y^0$  [12] pulse. The INEPT is implemented using  $90_y^0$  pulse followed by  $90_{-x}^0$  with  $\frac{1}{2J}$  time interval in between. The pseudo Hadamard gate ( $90_y^0$  pulse) is included in the INEPT sequence

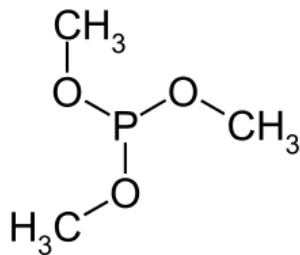


Figure 3.3: Structure of Tri-MethylPhosphite

Assuming all the spins in the star topology molecule are in the spin up ( $|0\rangle$ ) state, denoted by  $|0_P 0 \dots 0_{H}\rangle$ , where  $|0_P\rangle$  indicates the state of phosphorus and  $|00 \dots 0_H\rangle$  indicates the peripheral hydrogens. After INEPT is done,

the pseudo Hadamard operator, which is  $90_y^0$  pulse is applied to the central phosphorus spin. This will create a superposition state in the phosphorus spin, taking  $|0_P\rangle$  to  $\frac{1}{\sqrt{2}}(|0_P\rangle + |1_P\rangle)$ . The transformation can be given as:

$$|0_P 0 \dots 000_H\rangle \xrightarrow{90_y^0} \frac{1}{\sqrt{2}}(|0_P\rangle + |1_P\rangle) |00 \dots 000_H\rangle = \frac{1}{\sqrt{2}}(|0_P 00 \dots 000_H\rangle + |1_P 00 \dots 000_H\rangle) \quad (3.1)$$

After the pseudo Hadamard, C-NOT gate/operator, which is  $90_x^H - \frac{1}{2J} - 90_y^H$  is applied to the peripheral hydrogens (called target qubit), using the phosphorus state as the control. This C-NOT gate will flip the target qubit from  $|0\rangle$  to  $|1\rangle$  and  $|1\rangle$  to  $|0\rangle$ , if the control qubit is  $|1\rangle$ , but if the control qubit is in state  $|0\rangle$ , the C-NOT gate will not have any effect on the target qubits.

$$\frac{1}{\sqrt{2}}(|0_P 00 \dots 000_H\rangle + |1_P 00 \dots 000_H\rangle) \xrightarrow{C-NOT} \frac{1}{\sqrt{2}}(|0_P 00 \dots 000_H\rangle + |1_P 11 \dots 111_H\rangle) \quad (3.2)$$

This particular entangled state is called N00N state, which is maximally entangled state in MSSM. Since the system is in thermal equilibrium, all the spins are not in the  $|0\rangle$  state, other MSSM states are also generated by the pseudo Hadamard[12] and the C-NOT gates. To select out a particular state, or simply particular coherence, two selective gradients  $G_2$  and  $G_3 = -gG_2$  are applied, with  $g = \gamma_{eff}/\gamma_P$ , where

$$\gamma_{eff} = \gamma_P + (N - 1)\gamma_H \quad (3.3)$$

is the effective gyromagnetic ratio of particular MSSM state,  $N$  is the number of spins in the MSSM state,  $\gamma_P$  and  $\gamma_H$  are the gyromagnetic ratios of Phosphorus and proton. For uncoupled spins,  $N = 1$  and  $\gamma_{eff}$  reduces to  $\gamma_P$ . The larger the value of  $g$ , the more sensitive is the MSSM state and allows the study of diffusion with weaker PFGs and smaller durations ( $\Delta$ ) between the two gradients i.e the two  $G_1$ s.

### 3.1.1 Measurement of Diffusion Constant

As already mentioned in section 2.2.2, the Hahn echo signal is attenuated due to molecular diffusion and the relation between the signal intensity and the gradient strength is given in eqn(2.15). Taking the particular MSSM state, which is the N00N state. During the  $G_1 - \pi - G_1$  pulse sequence, the state

undergoing diffusion of a distance  $dz$  acquires a net relative phase  $d\phi$ [11]:

$$\frac{1}{\sqrt{2}}(|0_P00\dots000_H\rangle + |1_P11\dots111_H\rangle) \xrightarrow{G_1 - \pi - G_1} \frac{1}{\sqrt{2}}(|0_P00\dots000_H\rangle + e^{id\phi} |1_P11\dots111_H\rangle) \quad (3.4)$$

which can be given as:

$$d\phi = \gamma_{eff} dz G_1 \delta \quad (\delta = \text{duration of the field gradient}) \quad (3.5)$$

Since the MSSM state which we consider is a multiple quantum coherence, we need to convert it back to single quantum coherence for detection. This is done by the second C-NOT gate:

$$\frac{1}{\sqrt{2}}(|0_P00\dots000_H\rangle + e^{id\phi} |1_P11\dots111_H\rangle) \xrightarrow{C-NOT} \frac{1}{\sqrt{2}}(|0_P\rangle + e^{id\phi} |1_P\rangle) |00\dots000_H\rangle \quad (3.6)$$

In an ensemble of nuclei, the net relative phase acquired results in the signal attenuation. The diffusion constant can be determined using the equation given in eqn(2.15). From this, the diffusion constant can be given as:

$$D = -\frac{\text{slope}}{\gamma_{eff}^2 \delta^2 (\Delta - \frac{\delta}{3})} \quad (3.7)$$

Here, *slope* is the slope of the graph plot between  $\ln[S(t)]$  versus  $G_1^2$ .

### 3.1.2 Experimental part for Diffusion

The system under observation is  $10\mu L$  of Trimethyl-phosphite in  $600\mu L$  of liquid crystal EBBA. The diffusion experiment is carried out in 500 MHz Bruker NMR Spectrometer. In this molecule, the nine chemically equivalent  $^1H$  spins are equally coupled with the central  $^{31}P$ . Accordingly, the phosphorus spectrum splits into 10 lines as shown in fig 3.4:

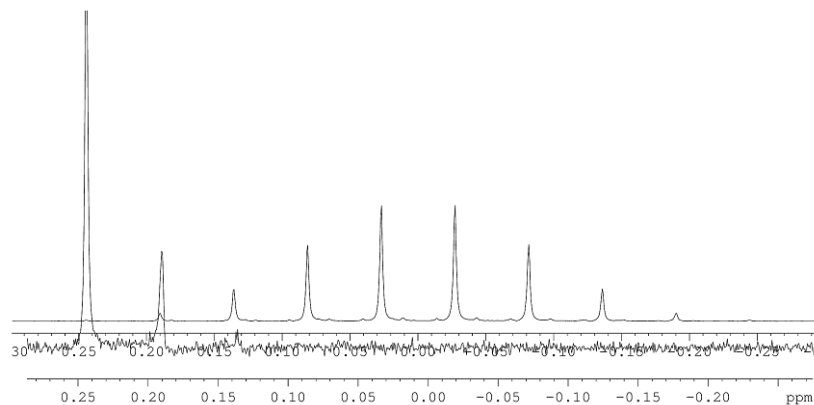


Figure 3.4: Spectrum of  $^{31}\text{P}$  in Tri-methylphosphite, the left most signal is of N00N state, since it decays extremely fast, we cannot study the diffusion parameters

The initial INEPT is to enhance the signal from  $^{31}\text{P}$  polarization as shown in fig 3.5.

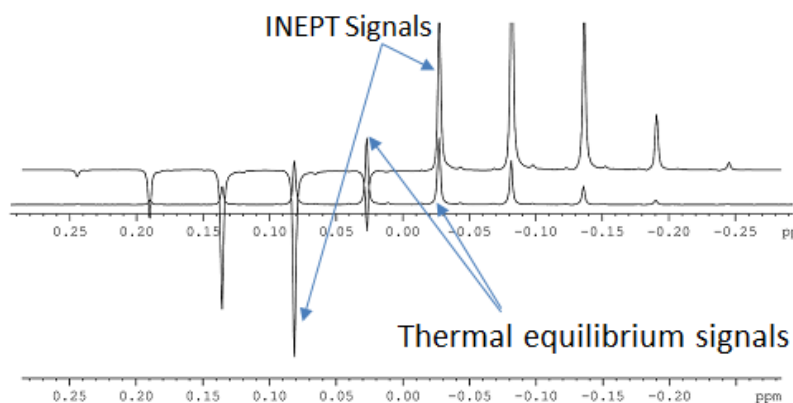


Figure 3.5: Signal of  $^{31}\text{P}$  with INEPT(upper peak) and without INEPT

First, the diffusion is carried out using the pulse sequence given in fig 2.3 by monitoring only the central  $^{31}\text{P}$ , and after that the diffusion of MSSM states are studied using the pulse sequence given in fig 3.2, the selective gradients  $G_2$  and  $G_3$  are adjusted using the relation  $G_3 = -gG_2$  ( $g = \gamma_{eff}/\gamma$ ) for selecting the desired MSSM state. The value of  $g$  for 2,4,6 and quantum coherences are given:

No. of coherence	2	4	6	8
g	3.47	8.41	13.35	18.29

Table 3.1: Ratio of selective gradients( $\frac{G_2}{G_1}$ ) w.r.t no. of coherences

Single quantum coherence does not require selective gradient since it is done using standard method given in fig 2.3 which is not suitable for entangled states.

### 3.2 Generating different N00N state in 22 spin system

N00N state is a quantum mechanical many-body entangled state. For an N number of spin  $\frac{1}{2}$  system, it is a superposition of N-spins being all down and all up. It can be represented as:

$$|\Psi_{N00N}\rangle = \frac{1}{\sqrt{2}}(|N_{\uparrow}, 0_{\downarrow}\rangle + |0_{\uparrow}, N_{\downarrow}\rangle) \quad (3.8)$$

The first term in the right hand side indicates N spins up, no spin down. The second one indicates no spin up, N spins down. Such a spin N00N state will acquire a phase factor  $e^{iN\delta t}$  [14] ( $\delta$  is the offset frequency in rotating frame), thus showing an  $N$ -fold increase in the phase acquired and hence a greater sensitivity to the applied field gradient. The N00N state concept has also been applied to create magnetic field sensors by Jones et al[14].

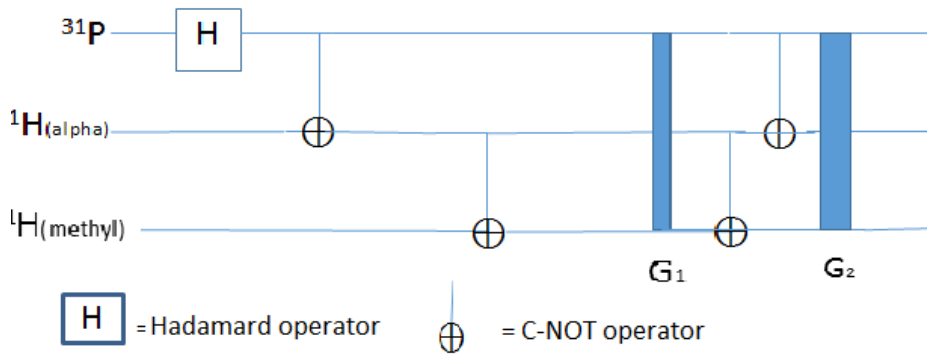


Figure 3.6: Circuit for N00N state in Tri-isopropyl-phosphite.  $G_1$  and  $G_2$  are the selective gradients

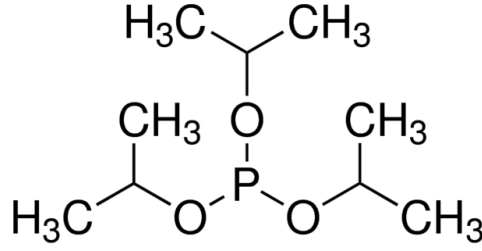


Figure 3.7: Triisopropyl Phosphite, molecule used for generating N00N states.

### 3.2.1 Experimental Part for N00N states

The molecule that is used to generate the N00N state in this experiment is tri-isopropylphosphite dissolved in DMSO solvent. It has one central  $^{31}\text{P}$ , 3  $\alpha$ - hydrogens and 18 methyl-hydrogens. This experiment had been done in a 600MHz Bruker NMR Spectrometer. The N00N states are generated for  $4(^{31}\text{P} + 3 \alpha - \text{H})$ ,  $5(^{31}\text{P} + 3 \alpha - \text{H} + 1 \text{Methyl} - \text{H})$ ... upto  $22(^{31}\text{P} + 3\alpha - \text{H} + 18 \text{Methyl} - \text{H})$  spin system. First, we demonstrate how spin polarization transfer from  $\alpha - \text{H}$  to  $^{31}\text{P}$  using INEPT enhances the signal from  $^{31}\text{P}$ . Since the  $\alpha - \text{H}$  and the Methyl Hydrogens are homonuclear species, while applying the Hadamard and C-NOT operators, a special type of RF pulses called "selective pulses" are used so that the operators can be applied specifically. Otherwise, if normal RF pulses are applied, it will excite both the Hydrogen species simultaneously which we want to avoid.

The ratio of the strength of the two selective gradients( $\frac{G_2}{G_1}$ ) are calculated using the formula:

$$\frac{G_2}{G_1} = \frac{\gamma_P + (N - 1)\gamma_H}{\gamma_P} \quad (3.9)$$

The numerator and the denominator can be multiplied with the strength of the external field( $B_o$ ) which is homogenous in time and space across the sample, since  $\gamma B_o$  gives the larmor frequency  $\omega_o$ , the equation becomes:

$$g = \frac{G_2}{G_1} = \frac{\omega_o^P + (N - 1)\omega_o^H}{\omega_o^P} \quad (3.10)$$

The spectrometer that was used in this experiment has a field of around 14.1 Tesla, under this, the larmor frequency of  $^1\text{H}(\omega_o^H)$  is 600.3 MHz and that of  $^{31}\text{P}(\omega_o^P)$  is 243.01 MHz(units are given in terms of Hertz and not in *radian s<sup>-1</sup>*). The numerical value of  $g$  calculated for different N00N states are given in tabular form :

No. of N00N(N)	4	5	6	7	8	9	10	11
g	8.41	10.88	13.35	15.82	18.29	20.76	23.23	25.7

No. of N00N(N)	12	13	14	15	16	17	18
g	28.17	30.64	33.11	35.58	38.05	40.52	42.99

No. of N00N(N)	19	20	21	22
g	45.46	47.94	50.41	52.88

Table 3.2: Ratio of selective gradients ( $\frac{G_2}{G_1}$ ) w.r.t no. of N00N

Due to instrumental limitations, the value of the strength of the selective gradients should be adjusted based on their respective value of  $g$  such that either of the gradient strength should not exceed 100.

### 3.2.2 Coherence selection by field gradients

To select a particular quantum coherence  $N$ , we deployed two selective gradients. The phase acquired is proportional to the number of quantum and the gradient as given

$$\phi_1 = \gamma_{eff} G_1 z \tau \quad (3.11)$$

$N$  is contained in  $\gamma_{eff}$ (eqn3.3),  $G_1$  is the first selective gradient.

The C-NOT operator between the two gradients convert the multiple quantum to single quantum coherence. In our experiment, the single quantum is on the  $^{31}P$ . The second gradient  $G_2$  contributes to an extra phase on the  $^{31}P$  given by:

$$\phi_2 = \gamma_P G_2 z \tau \quad (3.12)$$

To select a particular coherence  $N$ , we need to set  $\phi_1 = \phi_2$ , such that

$$\frac{\gamma_{eff}}{\gamma_P} = \frac{G_2}{G_1} \quad (3.13)$$

this cancels the phase acquired due to the first gradient and refocus the magnetization of the desired coherence.

# Chapter 4

## Results

Results of signal attenuation due to diffusion, calculation of diffusion constant from the experimental data and N00N state signals are given in this chapter.

### 4.1 Data of diffusion experiment

The diffusion of the molecules is monitored by the  $G_1$  gradient, the selective gradients,  $G_2$  and  $G_3$  are adjusted in such a way that only 1,2,4,6 and 8 quantum coherences are selected. Data acquisition is done only when the multiple quantum coherence is converted back into single quantum coherence on the central  $^{31}P$  by the final C-NOT gate.

Graphs of different quantum coherences, plot of  $\ln[S(t)]$  versus  $G_1^2$  are given:



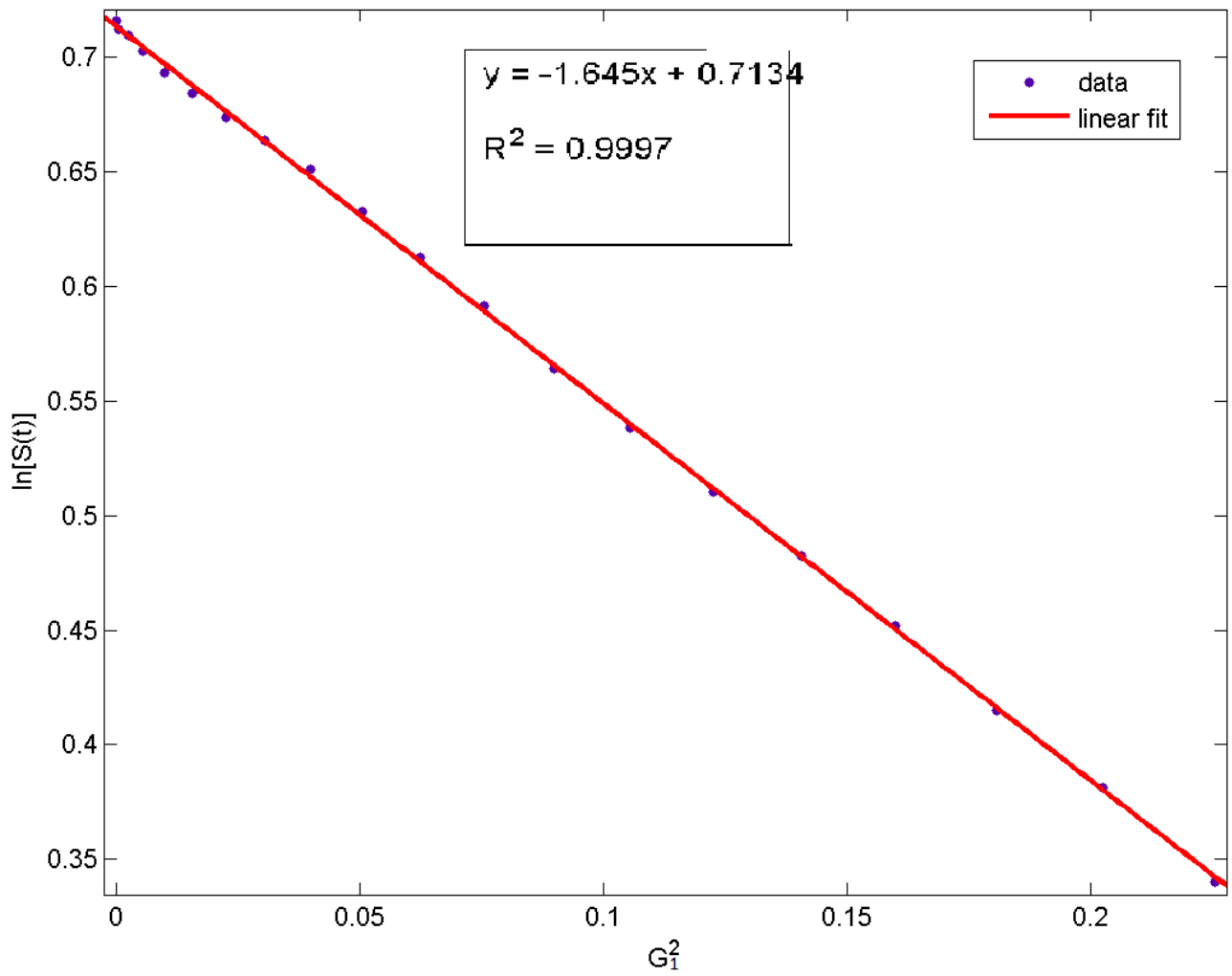


Figure 4.1: 1 quantum coherence,  $\Delta = 801ms$   
 $\delta = 1.5ms$ , slope =  $-1.645$

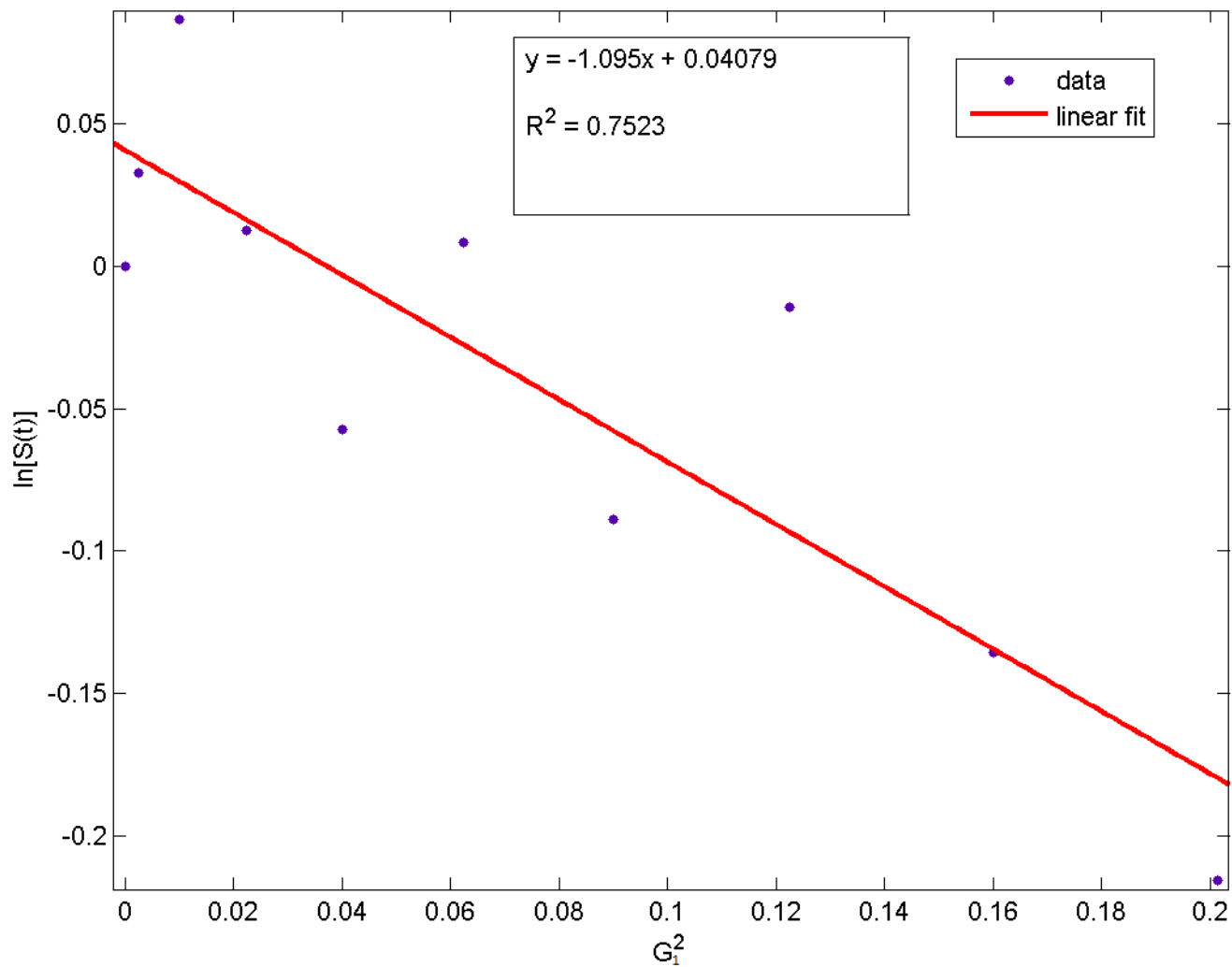


Figure 4.2: 2 quantum coherence,  $\Delta = 161ms$   
 $\delta = 1.5ms$ , slope =  $-1.095$

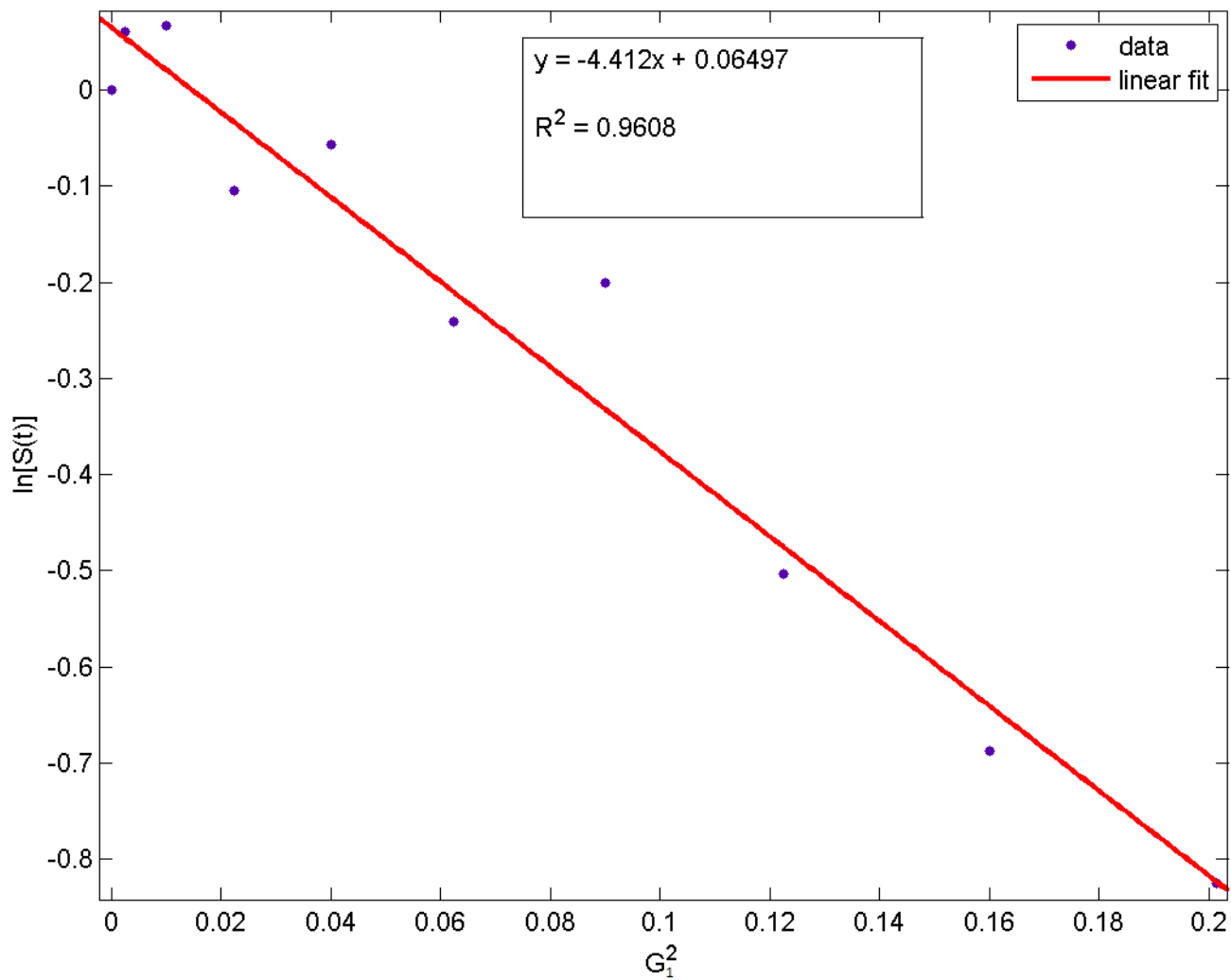


Figure 4.3: 4 quantum coherence,  $\Delta = 101ms$   
 $\delta = 1.5ms$ , slope =  $-4.412$

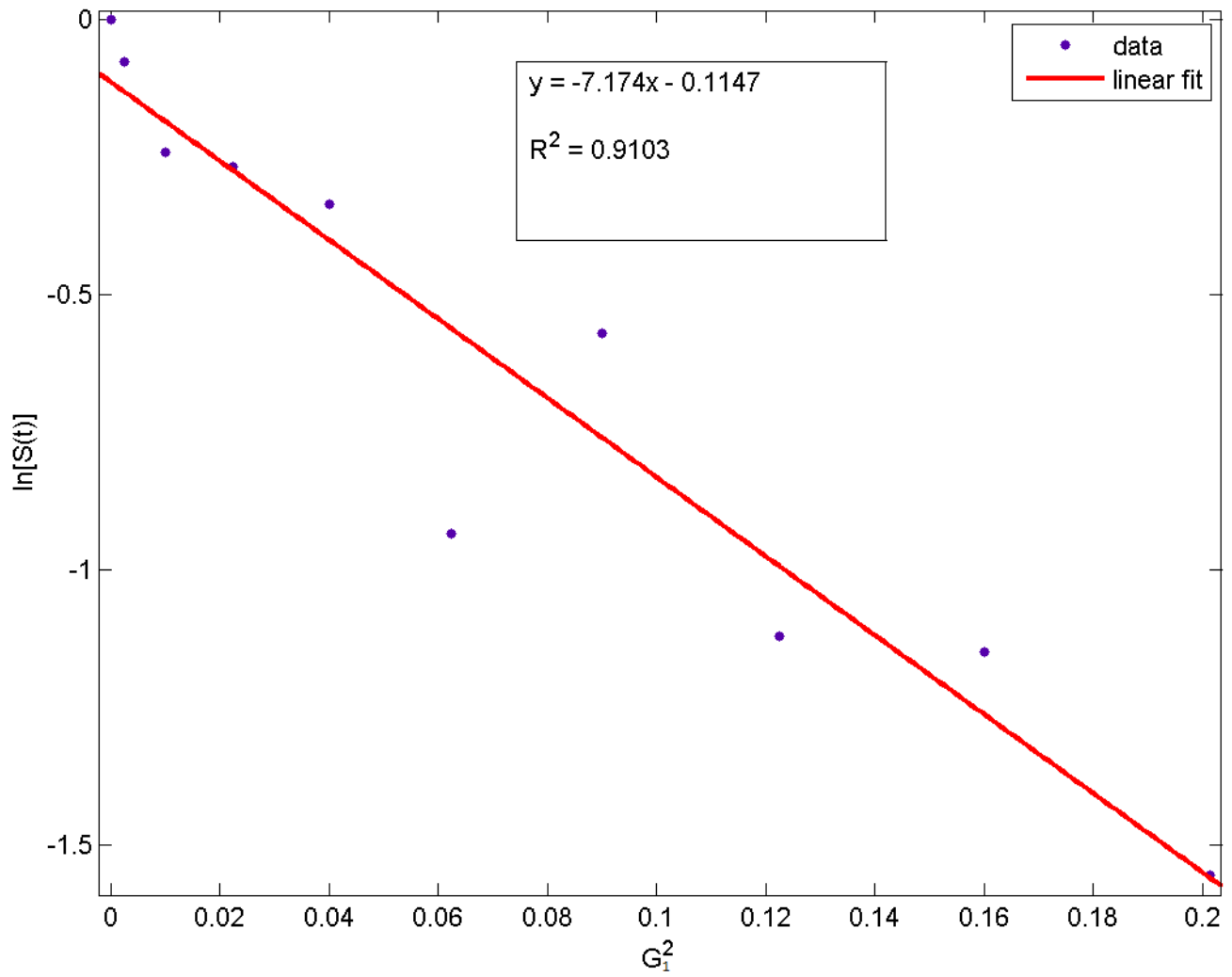


Figure 4.4: 6 quantum coherence,  $\Delta = 61ms$   
 $\delta = 1.5ms, slope = -7.174$

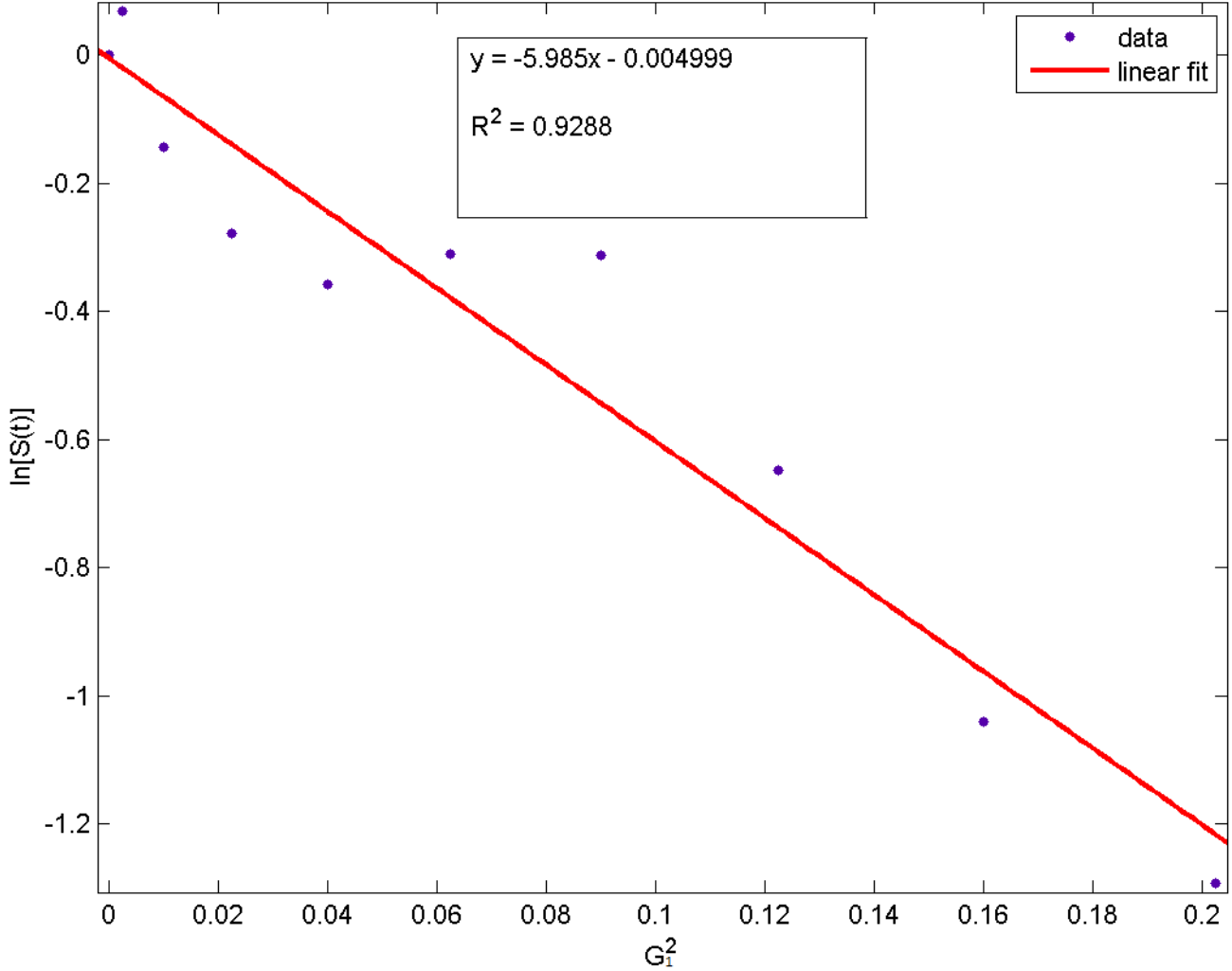


Figure 4.5: 8 quantum coherence,  $\Delta = 11ms$   
 $\delta = 1.5ms$ , slope =  $-5.985$

#### 4.1.1 Calculations of Diffusion constant for different quantum coherences

This is done using eqn(3.3)(for calculating  $\gamma_{eff}$  and eqn(3.7)(for finding D). For different quantum coherences, the calculation is given in the form of table( $\gamma_P = 1.08 \times 10^8 \text{ rad s}^{-1}T^{-1}$ ,  $\gamma_H = 2.67 \times 10^8 \text{ rad s}^{-1}T^{-1}$ ):

No. of quantum coherence(N)	slope	$\Delta(ms)$	$\delta(ms)$	$\gamma_{eff}(rad\ s^{-1}T^{-1})$	$D(m^2s^{-1})$
1	-1.645 fig(4.1)	801	1.5	$1.08 \times 10^8$	$0.7 \times 10^{-10}$
2	-1.095 fig(4.2)	161	1.5	$3.75 \times 10^8$	$0.2 \times 10^{-10}$
4	-4.412 fig(4.3)	101	1.5	$9.09 \times 10^8$	$0.2 \times 10^{-10}$
6	-7.174 fig(4.4)	61	1.5	$14.43 \times 10^8$	$0.2 \times 10^{-10}$
8	-5.985 fig(4.5)	11	1.5	$19.77 \times 10^8$	$0.6 \times 10^{-10}$

Table 4.1: Table of diffusion data

The single quantum coherence is done using the pulse sequence given in figure 2.3, which is also called the standard method. Since the solvent is liquid crystal, the 10 quantum coherence or the 10 N00N state is not selectable as the signal decays extremely fast.

## 4.2 Pulse sequence and Signal Spectrum of N00N states

Following figure shows the  $^{31}P$  spectrum and how INEPT enhances the signal:

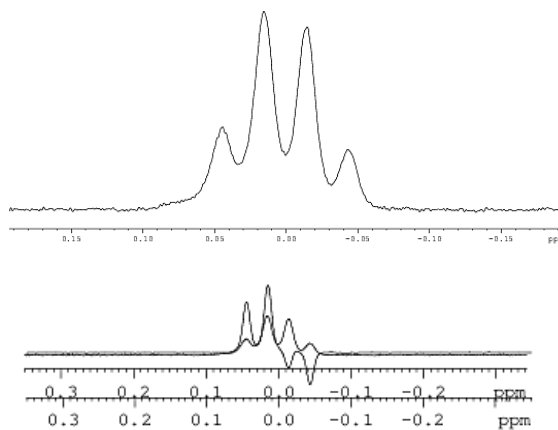


Figure 4.6: Phosphorus signal(upper), signal enhancement by INEPT(lower). The inverted peaks are due to the anti-phase term generated by INEPT pulses.

The RF pulse sequence and the signal spectrum of different N00N states are given:

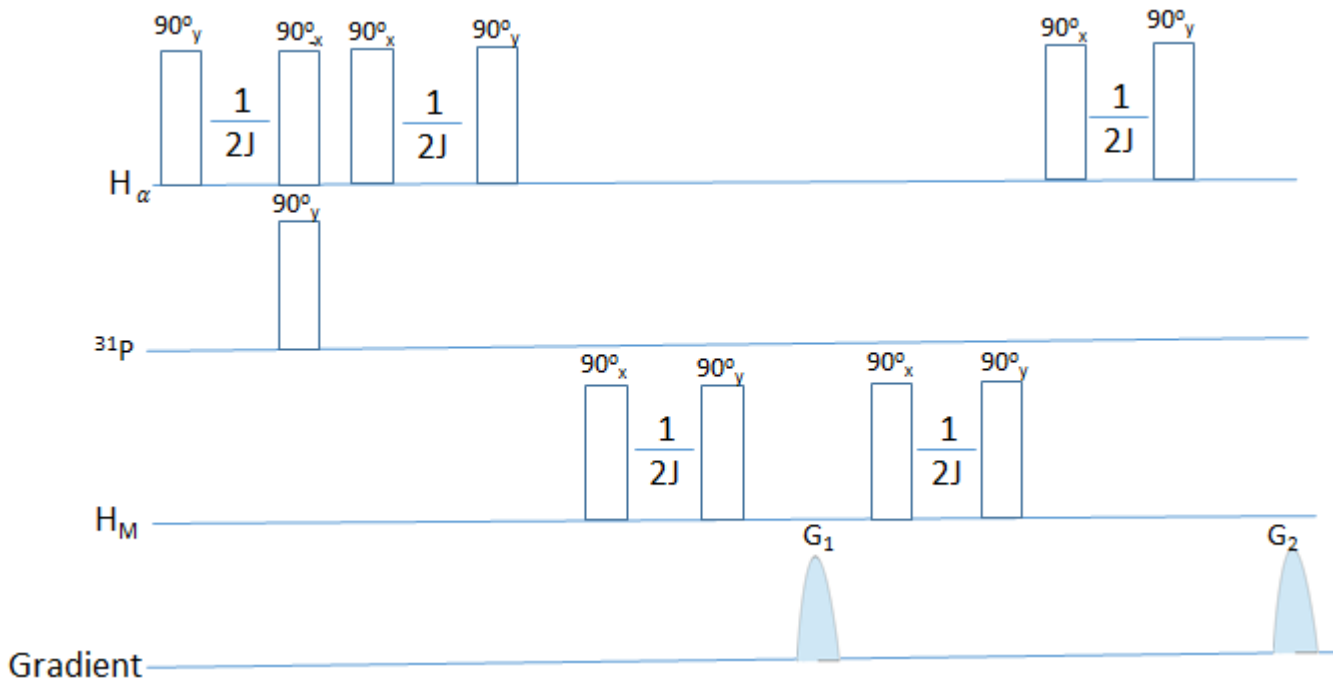


Figure 4.7: RF pulse sequence for generating NOON state,  $J$  denotes the  $J$  coupling frequency. The pseudo Hadamard operator ( $90_y^0$  pulse) is included in the INEPT

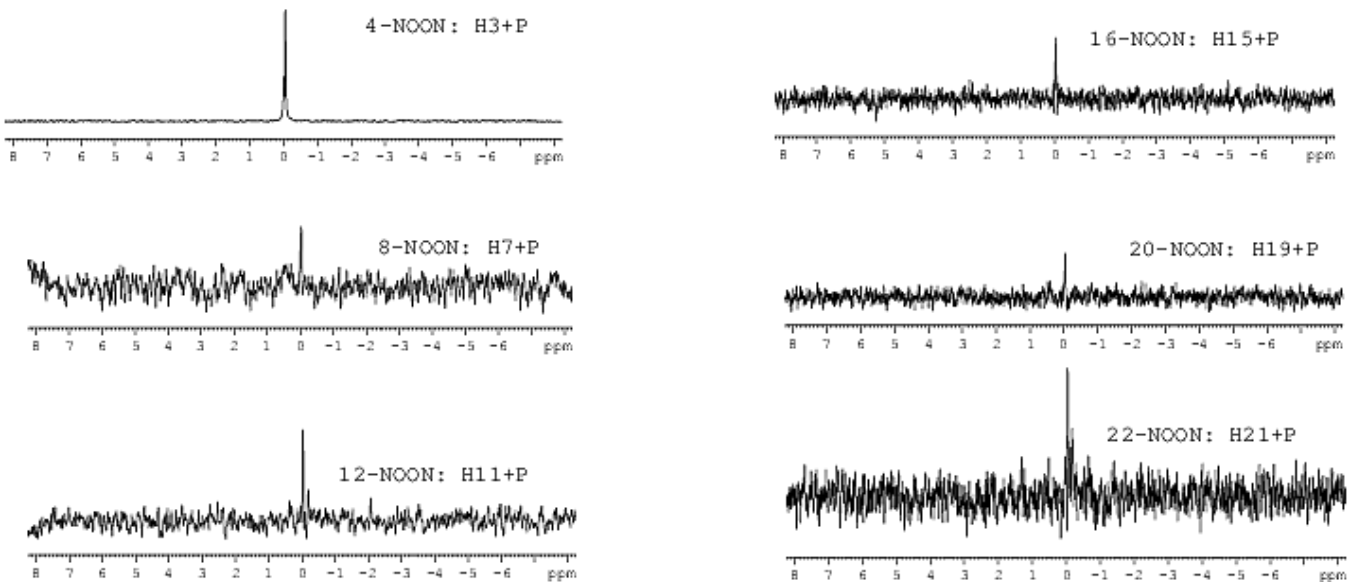


Figure 4.8: Different NOON states

# Chapter 5

## Discussion

Following are the discussions and conclusions made from the experiments.

### 5.1 Comparison between single quantum diffusion and multiple quantum diffusion

Single quantum uses the method given in fig 2.3, while the multiple quantum uses the method given in fig 3.1. If we carefully compare the two methods from the respective data, the multiple quantum method requires much lesser time compared to the single quantum method. This serves as a great advantage over the single quantum method, when dealing with molecules which have extremely short relaxation time because we can probe the decay of the signal in much shorter time. Also, the multiple quantum method is extremely useful for studying slow diffusion since it requires much lesser time.

### 5.2 N00N states

We have shown how INEPT technique enhances the NMR signal by transferring the spin polarization from more sensitive nucleus to lesser sensitive nucleus(fig 4.6(lower)). In generating different N00N states, since the molecule that was used has two types of hydrogen species( $\alpha - H$  and Methyl-H), both of which are homogenous nuclei, we cannot use the normal RF pulse, specially for C-NOT to selectively excite the two hydrogen species. For that, we deployed a particular type of selective RF pulse called "*bang-bang pulses*", which is far more efficient than its counterpart "*GRAPE pulses*". Using this "*bang-bang pulses*", we generated a 22 spin N00N system successfully(fig 4.8(bottom right)).



# References

- [1] E. L. Hahn, Spin echoes, *Physical Review* 80 (1950) 580–594.
- [2] E. o. STE]SKALt, J. E. TANNER, Spin diffusion measurements: Spin echoes in the presence of a time-dependent field gradient, *The Journal of Chemical Physics* 42 (1964) 288–292.
- [3] R. Ghez, Diffusion phenomena : Cases and studies, in: *Diffusion Phenomena*, Springer, 2001.
- [4] Diffusion measurements by nuclear magnetic resonance (nmr).  
URL [http://www.uni-muenster.de/imperia/md/content/physikalische\\_chemie/nmr\\_pfg\\_diffusion.pdf](http://www.uni-muenster.de/imperia/md/content/physikalische_chemie/nmr_pfg_diffusion.pdf)
- [5] [link].  
URL [http://en.wikipedia.org/wiki/Einstein\\_relation\\_%28kinetic\\_theory%29#Stokes-Einstein\\_equation](http://en.wikipedia.org/wiki/Einstein_relation_%28kinetic_theory%29#Stokes-Einstein_equation)
- [6] [link].  
URL [http://en.wikipedia.org/wiki/Stokes%27\\_law](http://en.wikipedia.org/wiki/Stokes%27_law)
- [7] W. S. Price, P. W. Kuchell, Effect of nonrectangular field gradient pulses in the stejskal and tanner (diffusion) pulse sequence, *Journal of Magnetic Resonance* 94 (1991) 133–139.
- [8] H. Y. Carr, E. M. Purcell, Effects of diffusion on free precession in nuclear magnetic resonance experiments, *Physical Review* 94 (1954) 630–638.
- [9] W. S. Price, Pulsed-field gradient nuclear magnetic resonance as a tool for studying translational diffusion: Part 1. basic theory.  
URL <http://onlinelibrary.wiley.com/doi/10.1002/%28SICI%291099-0534%281997%299:5%3C299::AID-CMR2%3E3.0.CO;2-U/epdf>

- [10] C. S. Johnson Jr, Diffusion ordered nuclear magnetic resonance spectroscopy: principles and applications), Progress in Nuclear Magnetic Resonance Spectroscopy 34 (1999) 203–256.
- [11] A. Shukla, M. Sharma, T. S. Mahesh, Noon states in star-topology spin-systems: Applications in diffusion studies and rf inhomogeneity mapping, Chemical Physics Letters 592 (2014) 227–231.
- [12] J. A. Jones, R. H. Hansen, M. Mosca, Quantum logic gates and nuclear magnetic resonance pulse sequences, Journal of magnetic Resonance 135 (1998) 353–360.
- [13] G. Bodenhausenl, Multiple quantum nmr, Progress in NMR Spectroscopy 14 (1981) 137.
- [14] J. A. Jones et al, Magnetic field sensing beyond the standard quantum limit using 10-spin noon states, SCIENCE 324 (2009) 1166–1168.
- [15] M. H. Levitt, in: Spin Dynamics: Basics of Nuclear Magnetic Resonance, Wiley, 2002, pp. 282–284.
- [16] J. Keeler, Product operators, in: Understanding NMR Spectroscopy(2<sup>nd</sup> edition), Wiley, 2010.
- [17] R. Freemam, G. A. Morris, Enhancement of nuclear magnetic resonance signals by polarization transfer, Journal of the American Chemical Society 101:3 (1979) 760–762.
- [18] [link].  
URL [http://en.wikipedia.org/wiki/Insensitive\\_nuclei\\_enhanced\\_by\\_polarization\\_transfer](http://en.wikipedia.org/wiki/Insensitive_nuclei_enhanced_by_polarization_transfer)

# Appendix A

## Long proofs

### A.1 Proof of Hahn Echo described in Sec 2.1.2 using product operator formalism

For a spin  $\frac{1}{2}$  system, the product operator formalism requires the involvement of density matrix. In thermal equilibrium at temperature  $T$  in the presence of external magnetic field  $B_o$ , the population of Zeeman states obey the *Boltzmann distribution*[15]:

$$\rho_{eq} = \frac{\exp(-\hbar\omega_r/k_B T)}{\sum_s \exp(-\hbar\omega_s/k_B T)} \quad (\text{A.1})$$

where  $k_B = 1.38066 \times 10^{-23} JK^{-1}$  is the *Boltzmann constant*.

The *Boltzmann distribution* causes the lower energy eigenstates to be more populated than the higher energy eigenstates and the energy difference between the Zeeman states is about four orders of magnitude smaller than the available thermal energy. Since the thermal equilibrium population difference between the states is very small, it is possible to simplify eqn(A.1) by using some approximations.

By defining the *Boltzmann factor*  $\Omega = \frac{\hbar\gamma B_o}{k_B T}$ , the exponential factors in eqn A.1 can be written as follows:

$$\exp(-\hbar\omega_\alpha/k_B T) = \exp\left(\frac{\Omega}{2}\right) \quad (\text{A.2})$$

$$\exp(-\hbar\omega_\beta/k_B T) = \exp\left(-\frac{\Omega}{2}\right) \quad (\text{A.3})$$

where  $\alpha$  corresponds to spin up  $|0\rangle$  state and  $\beta$  corresponds to spin down  $|1\rangle$ ,  $\hbar\omega_\alpha = -\hbar\gamma B_o$ ,  $\hbar\omega_\beta = \hbar\gamma B_o$ . Since the factor  $\Omega$  is a very small number. It

is possible to expand the above exponentials as a power series and take only the first two term terms:

$$\exp(-\hbar\omega_\alpha/k_B T) = 1 + \frac{\Omega}{2} \quad (\text{A.4})$$

$$\exp(-\hbar\omega_\beta/k_B T) = 1 - \frac{\Omega}{2} \quad (\text{A.5})$$

The denominator of eqn(A.1) can also be written as:

$$\exp(-\hbar\omega_\alpha/k_B T) + \exp(-\hbar\omega_\beta/k_B T) = 2 \quad (\text{A.6})$$

Therefore, the thermal equilibrium populations of the two states are:

$$\rho_{|0\rangle}^{eq} = \frac{1}{2}\left(1 + \frac{\Omega}{2}\right) = \frac{1}{2} + \frac{B}{4} \quad (\text{A.7})$$

$$\rho_{|1\rangle}^{eq} = \frac{1}{2}\left(1 - \frac{\Omega}{2}\right) = \frac{1}{2}\left(1 - \frac{B}{4}\right) \quad (\text{A.8})$$

The above approximation is called the *high-temperature approximation*. For positive  $\gamma$ , the low-energy state  $|0\rangle$  is more populated slightly than the high-energy state  $|1\rangle$ . Physically, this means that in thermal equilibrium, there is a net polarization of the magnetic moment vectors along the direction of the external magnetic field. Therefore, the thermal equilibrium density matrix for isolated spin  $\frac{1}{2}$  is given by:

$$\rho_{eq} = \begin{bmatrix} \frac{1}{2} + \frac{\Omega}{4} & 0 \\ 0 & \frac{1}{2} - \frac{\Omega}{4} \end{bmatrix} \quad (\text{A.9})$$

In terms of angular momentum operators, this corresponds to:

$$\hat{\rho}_{eq} = \frac{1}{2}\hat{1} + \frac{\Omega}{2}\hat{I}_z \quad (\text{A.10})$$

where  $\hat{1}$  is the identity matrix and  $\hat{I}_z$  is the  $z$  - component of the total spin angular momentum and is represented by  $\hat{I}_z = \frac{\hbar}{2}\sigma_z$ ,  $\sigma_z$  is the Pauli  $z$  operator. The hat ( $\hat{\quad}$ ) indicates they are operators. This thermal equilibrium density operator forms the starting point for subsequent calculations.

The function of RF pulses is to rotate the equilibrium magnetization which is represented by eqn(A.10). For the calculations, we can omit the first part of eqn(A.10) since it is identity and any operator acting on it has no effect, the rotation dynamics happens on the second part. At time  $t = 0$ , i.e before no RF pulse is applied, density operator is given by  $\rho(0)$  eqn(A.10). When an on resonance RF pulse is applied, it rotates the density operator

to some angle  $\beta$ , in terms of mathematical equation, this rotation can be represented as:

$$\rho(t) = \exp(-i\beta\hat{I}_k)\rho(0)\exp(i\beta\hat{I}_k) \quad (\text{A.11})$$

Here,  $\hat{I}_k$  represents the direction of the RF pulse (k can be x, y and z) and  $\beta$  is the flip angle, i.e the amount in which the density operator is rotated. In terms of angular momentum eqn(A.11) can be represented as:

$$\hat{I}_z(t) = \exp(-i\beta\hat{I}_k)\hat{I}_z(0)\exp(i\beta\hat{I}_k) = \cos(\beta)\hat{I}_z + \sin(\beta)(\text{new operator}) \quad (\text{A.12})$$

The above equation is true only when the phase of the RF pulse applied is different from the operator in the LHS and the *new operator* comes from the cross product of  $\hat{I}_x$ ,  $\hat{I}_y$  and  $\hat{I}_z$ . For more convenience, in product operator formalism, eqn(A.12) can be written as[16]:

$$\hat{I}_z \xrightarrow{\beta\hat{I}_k} \cos(\beta)\hat{I}_z + \sin(\beta)(\text{new operator}) \quad (\text{A.13})$$

The arrow along with  $\beta\hat{I}_k$  is called propagator and is equivalent to the middle term in eqn(A.12).

Now, coming to the Hahn Echo, the pulse sequence is already given in fig. 2.1. Starting from equilibrium, a  $\frac{\pi}{2}$   $x$ - pulse is applied to  $\hat{I}_z$ . Using product operator method, this can be written as:

$$\hat{I}_z \xrightarrow{\frac{\pi}{2}\hat{I}_x} \cos\left(\frac{\pi}{2}\right)\hat{I}_z + \sin\left(\frac{\pi}{2}\right)(-\hat{I}_y) = -\hat{I}_y \quad (\text{A.14})$$

This implies a  $\frac{\pi}{2}$   $x$  pulse rotates  $\hat{I}_z$  to  $-\hat{I}_y$ , since vector cross product of  $x$  and  $z$  gives  $-y$ . Now, during the free evolution of time duration  $\tau$ ,  $-\hat{I}_y$  evolves under the chemical shift Hamiltonian  $H = \omega\hat{I}_z$  as:

$$-\hat{I}_y \xrightarrow{\omega\hat{I}_z\tau} -\cos(\omega\tau)\hat{I}_y + \sin(\omega\tau)\hat{I}_x \quad (\text{A.15})$$

The above equation tells that the magnetization vector precess in the transverse plane with a chemical shift frequency  $\omega$ . Next, a  $\pi$   $x$  pulse is applied, only the first term is affected since  $x$ - pulse on  $\hat{I}_x$  has no effect, it will remain as it is. So the effect of  $\pi$   $x$  pulse on  $-\cos(\omega\tau)\hat{I}_y$  is  $\cos(\omega\tau)\hat{I}_y$  (the  $\sin(\pi)$  term vanishes) and the net effect is given as:

$$-\cos(\omega\tau)\hat{I}_y + \sin(\omega\tau)\hat{I}_x \xrightarrow{\pi\hat{I}_x} \cos(\omega\tau)\hat{I}_y + \sin(\omega\tau)\hat{I}_x \quad (\text{A.16})$$

After the next free evolution of duration  $\tau$ , the magnetization vector refocus to  $\hat{I}_y$  and Hahn Echo is achieved:

$$\begin{aligned} \cos(\omega\tau)\hat{I}_y + \sin(\omega\tau)\hat{I}_x &\xrightarrow{\omega\hat{I}_z\tau} \cos^2(\omega\tau)\hat{I}_y - \cos(\omega\tau)\sin(\omega\tau)\hat{I}_x \\ &\quad + \sin(\omega\tau)\cos(\omega\tau)\hat{I}_x + \sin^2(\omega\tau)\hat{I}_y \end{aligned} \quad (\text{A.17})$$

The two middle terms of the last equation cancels each other and the remaining terms become  $\cos^2(\omega\tau)\hat{I}_y + \sin^2(\omega\tau)\hat{I}_y = \hat{I}_y$ , thus Hahn Echo is achieved.

## A.2 Effect of Pulse Field Gradient on Hahn Echo in presence of diffusion

In this section, the effect of Pulse Field Gradient(PFG) on Hahn Echo in the presence of spin diffusion is studied using product operator method. The pulse sequence for PFG is given in fig 2.3. A time delay of equal duration  $\tau$  is set between each and every pulse. Starting from the equilibrium, a  $\frac{\pi}{2}$   $x$ -pulse is applied which rotates  $\hat{I}_z$  to  $-\hat{I}_y$  eqn(A.14). Durin the first free evolution,  $-\hat{I}_y$  evolves under free Hamiltonian  $H = \omega\hat{I}_z\tau$  as:

$$-\hat{I}_y \xrightarrow{\omega\hat{I}_z\tau} -\cos(\omega\tau)\hat{I}_y + \sin(\omega\tau)\hat{I}_x \quad (\text{A.18})$$

Then the first gradient which has Hamiltonian of the form  $H = -\gamma gz\hat{I}_z$ [8] of duration  $\delta$  is applied. Here  $\gamma gz$  is the angular frequency of precession due to the gradient(let us denote by  $\nu$ , and  $g$  is the gradient strength), since gradient is along the  $z$  direction and  $gz$  is the field experienced due to the gradient by the spin at a distance  $z$  from some reference point in the sample:

$$\cos(\omega\tau)\hat{I}_y + \sin(\omega\tau)\hat{I}_x \xrightarrow{\nu\hat{I}_z\delta} \sin(\omega\tau + \nu\delta)\hat{I}_x - \cos(\omega\tau + \nu\delta)\hat{I}_y \quad (\text{A.19})$$

where  $\nu\delta$  is the extra phase acquired due to the field gradient. Before the application of  $\pi$   $x$  pulse, the magnetization undergoes second free evolution of duration  $\tau$ :

$$\begin{aligned} \sin(\omega\tau + \nu\delta)\hat{I}_x - \cos(\omega\tau + \nu\delta)\hat{I}_y &\xrightarrow{\omega\hat{I}_z\tau} \sin(2\omega\tau + \nu\delta)\hat{I}_x \\ &\quad - \cos(2\omega\tau + \nu\delta)\hat{I}_y \end{aligned} \quad (\text{A.20})$$

On the application of  $\pi$   $x$  pulse, the *sine* term with  $\hat{I}_x$  remains intact and only the *cosine* term is affected:

$$\begin{aligned} \sin(2\omega\tau + \nu\delta)\hat{I}_x - \cos(2\omega\tau + \nu\delta)\hat{I}_y &\xrightarrow{\pi\hat{I}_z} \sin(2\omega\tau + \nu\delta)\hat{I}_x \\ &\quad + \cos(2\omega\tau + \nu\delta)\hat{I}_y \end{aligned} \quad (\text{A.21})$$

During the third free evolution:

$$\begin{aligned} \sin(2\omega\tau + \nu\delta)\hat{I}_x + \cos(2\omega\tau + \nu\delta)\hat{I}_y &\xrightarrow{\omega\hat{I}_z\tau} \sin(2\omega\tau + \nu\delta - \omega\tau)\hat{I}_x \\ &\quad + \cos(2\omega\tau + \nu\delta - \omega\tau) \end{aligned} \quad (\text{A.22})$$

The right hand side can be written as:

$$\begin{aligned} \sin(2\omega\tau + \nu\delta - \omega\tau)\hat{I}_x + \cos(2\omega\tau + \nu\delta - \omega\tau) &= \sin(\omega\tau + \nu\delta)\hat{I}_x \\ &+ \cos(\omega\tau + \nu\delta)\hat{I}_y \end{aligned} \quad (\text{A.23})$$

Now, during the free evolution time, if the spin undergoes longitudinal diffusion of distance  $dz$ , on the application of second gradient, the extra phase acquired due to the first field gradient is not cancelled by the second gradient:

$$\begin{aligned} \sin(\omega\tau + \nu\delta)\hat{I}_x + \cos(\omega\tau + \nu\delta)\hat{I}_y &\xrightarrow{\nu'I_z\delta} \sin(\omega\tau + \nu\delta - \nu'\delta)\hat{I}_x \\ &+ \cos(\omega\tau + \nu\delta - \nu'\delta)\hat{I}_y \end{aligned} \quad (\text{A.24})$$

Here,  $\nu'\delta$  is the phase acquired due to the second field gradient. After the free evolution of duration  $\tau$ , the magnetization evolves as:

$$\begin{aligned} \sin(\omega\tau + \nu\delta - \nu'\delta)\hat{I}_x + \cos(\omega\tau + \nu\delta - \nu'\delta)\hat{I}_y &\xrightarrow{\omega I_z \tau} \sin(\omega\tau + \nu\delta - \nu'\delta)\cos(\omega\tau)\hat{I}_x \\ &- \cos(\omega\tau + \nu\delta - \nu'\delta)\sin(\omega\tau)\hat{I}_x \\ &+ \sin(\omega\tau + \nu\delta - \nu'\delta)\sin(\omega\tau)\hat{I}_y \\ &+ \cos(\omega\tau + \nu\delta - \nu'\delta)\cos(\omega\tau)\hat{I}_y \end{aligned} \quad (\text{A.25})$$

Now, using trigonometric relations the RHS becomes :

$$\sin(\omega\tau + \nu\delta - \nu'\delta - \omega\tau)\hat{I}_x + \cos(\omega\tau + \nu\delta - \nu'\delta - \omega\tau)\hat{I}_y \quad (\text{A.26})$$

The above equation can be further simplified, since the phase term due to chemical shift Hamiltonian cancels each other:

$$\sin(\nu\delta - \nu'\delta)\hat{I}_x + \cos(\nu\delta - \nu'\delta)\hat{I}_y \quad (\text{A.27})$$

As we can see, the  $\pi$  pulse cancels the evolution due to chemical shift Hamiltonian, if the spins retain their position (no diffusion) throughout the pulse sequence, the phase contribution due to the first and second gradient cancels each other, since both gradients contribute equal phase ( $\nu\delta = \nu'\delta$ ). The *sine* term vanishes and the *cosine* term remains, thus in absence of diffusion, complete Hahn Echo is achieved. However, due to spin diffusion, the phase contribution due to the two gradients do not cancel each other and complete Hahn Echo cannot be achieved and as a result, the Hahn Echo signal intensity is reduced.

## A.3 Inensitive Nuclei Enhanced by Polarization Transfer(INEPT)

Inensitive Nuclei Enhanced by Polarization Transfer(INEPT) is a signal enhancement method used in NMR which involves the transfer of nuclear spin polarization from spins with large gyromagnetic ratios( $\gamma$ ) to spins lower gyromagnetic ratios. The INEPT pulse sequence was proposed by Ray Freeman and Gareth A. Morris in 1979[17]. It uses J-coupling for the polarization transfer. This method is applied in generating the NOON state.

### A.3.1 Background

The NMR signal depends heavily on  $\gamma$ , nucleus with higher  $\gamma$  are easier or more sensitive for detection compared to nucleus with lower  $\gamma$ . The signal intensity from the nucleus of gyromagnetic ratio  $\gamma$  is proportional to  $\gamma^3$ [18] because the magnetic moment, Larmor frequency and Boltzmann populations depend on  $\gamma$ . For example, the gyromagnetic ratio of  $^1H$  ( $\gamma_H$ ) is four times that of  $^{13}C$  ( $\gamma_C$ ), this means  $^1H$  is 64 times more sensitive than  $^{13}C$ . Therefore, sensitivity enhancement technique is essential when acquiring NMR signal from insensitive nucleus.

### A.3.2 INEPT technique

The pulse sequence for INEPT is given as:

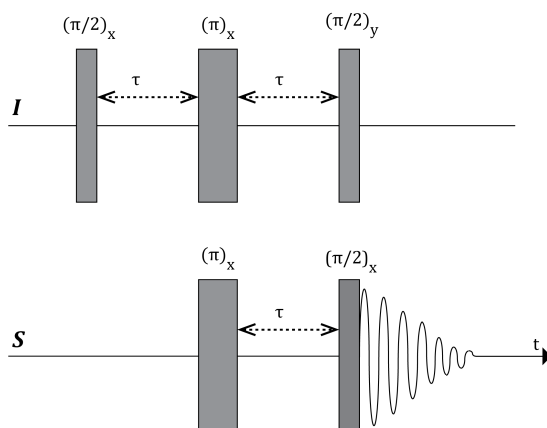


Figure A.1: INEPT Pulse Sequence. I and S denote the nucleus.  
 source:[http://en.wikipedia.org/wiki/Insensitive\\_nuclei\\_enhanced\\_by\\_polarization\\_transfer#/media/File:INEPT\\_Pulse\\_Sequence.png](http://en.wikipedia.org/wiki/Insensitive_nuclei_enhanced_by_polarization_transfer#/media/File:INEPT_Pulse_Sequence.png)



Using product operator method and starting from equilibrium on the  $I$  spin i.e  $\hat{I}_z$ , after the  $\frac{\pi}{2}$  pulse,  $\hat{I}_z$  evolved to  $-\hat{I}_y$ . When the pulse is switch off, the spins precess under the  $J$ -coupling Hamiltonian  $H = 2\pi J\hat{I}_z\hat{S}_z$  :

$$-\hat{I}_y \xrightarrow{2\pi J\hat{I}_z\hat{S}_z\tau} -\cos(\pi J\tau)\hat{I}_y + \sin(\pi J\tau)2\hat{I}_x\hat{S}_z \quad (\text{A.28})$$

After this,  $\pi$   $x$ -pulse is applied on both spins simultaneously:

$$-\cos(\pi J\tau)\hat{I}_y + \sin(\pi J\tau)2\hat{I}_x\hat{S}_z \xrightarrow{\pi\hat{I}_x+\hat{S}_x} \cos(\pi J\tau)\hat{I}_y - \sin(\pi J\tau)2\hat{I}_x\hat{S}_z \quad (\text{A.29})$$

During the second  $J$ -coupling evolution, the spins evolve as:

$$\begin{aligned} \cos(\pi J\tau)\hat{I}_y - \sin(\pi J\tau)2\hat{I}_x\hat{S}_z &\xrightarrow{2\pi J\hat{I}_z\hat{S}_z\tau} [\cos^2(\pi J\tau) - \sin^2(\pi J\tau)]\hat{I}_y \\ &\quad - 2\sin(\pi J\tau)\cos(\pi J\tau)2\hat{I}_x\hat{S}_z \end{aligned} \quad (\text{A.30})$$

Finally, a  $\frac{\pi}{2}$   $y$ -pulse is applied on  $I$  spin and  $\frac{\pi}{2}$   $x$ -pulse on  $S$  spin to transfer the spin polarization from  $I$  to  $S$ :

$$\begin{aligned} [\cos^2(\pi J\tau) - \sin^2(\pi J\tau)]\hat{I}_y - 2\sin(\pi J\tau)\cos(\pi J\tau)2\hat{I}_x\hat{S}_z &\xrightarrow{\frac{\pi}{2}\hat{I}_y+\frac{\pi}{2}\hat{S}_x} [\cos^2(\pi J\tau) \\ &\quad - \sin^2(\pi J\tau)]\hat{I}_y - 2\sin(\pi J\tau)\cos(\pi J\tau)2\hat{I}_z\hat{S}_y \end{aligned} \quad (\text{A.31})$$

As we can see, the spin polarization of  $\hat{I}_x$  from the anti-phase term  $2\hat{I}_x\hat{S}_z$  in eqn(A.30) is transferred to the  $S$  spin giving rise to the anti-phase term  $2\hat{I}_z\hat{S}_y$  in eqn(A.31). But in actual experiments, the two middle  $\pi$  pulses in the pulse sequence are not deployed, since we are on resonant with both the spins, only  $90_x^0$  and  $90_y^0$  pulses are deployed.

## A.4 List of figures and tables

1. Hahn Echo : figures 2.1 and 2.2
2. Standard Pulse sequence and pictorial illustration of Hahn Echo : figure 2.3 and 2.4
3. Circuit for generating multiple quantum coherence(for diffusion) : figure 3.1, Pulse sequence : figure 3.2 and N00N state : figure 3.6, Pulse sequence : figure 4.7
4. INEPT pulse sequence : figure A.1
5. Structures of trimethylphosphite : figure 3.3 and triisopropylphosphite : figure 3.7

6. Graph plots for diffusion data : figure 4.1 to figure 4.5
7. Signals of Phosphorus in trimethylphosphite : figure 3.4 and figure 3.5 and triisopropylphosphite : figure 4.6
8. Signals of different N00N state in triisopropylphosphite : figure 4.8
9. Tables : 3.1 and 3.2(Value of coherence selection gradients), diffusion data 4.1